Epoxyalkyl glycosides of D-xylose and xylo-oligosaccharides are active-site markers of xylanases from glycoside hydrolase family 11, not from family 10

Patricia NTARIMA*, Wim NERINCKX*, Klaus KLARSKOV†, Bart DEVREESE†, Mahalingeshwara K. BHAT‡, Jozef VAN BEEUMEN† and Marc CLAEYSSENS*[1]

*Laboratory for Biochemistry, Department of Biochemistry, Physiology and Microbiology, University of Ghent, K. L. Ledeganckstraat 35, B-9000 Ghent, Belgium, †Laboratory for Protein Biochemistry and Protein Engineering, Department of Biochemistry, Physiology and Microbiology, University of Ghent, K. L. Ledeganckstraat 35, B-9000 Ghent, Belgium, and ‡Institute for Food Research, Norwich Laboratory, Norwich Research Park, Colney, Norwich NR4 7UA, U.K.

A series of ω-epoxyalkyl glycosides of D-xylopyranose, xylobiose and xylotriose were tested as potential active-site-directed inhibitors of xylanases from glycoside hydrolase families 10 and 11. Whereas family-10 enzymes (*Thermoascus aurantiacus* Xyn and *Clostridium thermocellum* Xyn Z) are resistant to electrophilic attack of active-site carboxyl residues, glycoside hydrolases of family 11 (*Thermomyces lanuginosus* Xyn and *Trichoderma reesei* Xyn II) are irreversibly inhibited. The apparent inactivation and association constants (k_i, $1/K_i$) are one order of magnitude higher for the xylobiose and xylotriose derivatives. The effects of the aglycone chain length can clearly be described. Xylobiose and n-alkyl β-D-xylopyranosides are competitive ligands and provide protection against inactivation. MS measurements showed 1:1 stoichiometries in most labelling experiments. Electrospray ionization MS/MS analysis revealed the nucleophile Glu^{86} as the modified residue in the *T. lanuginosus* xylanase when 2,3-epoxypropyl β-D-xylopyranoside was used, whereas the acid/base catalyst Glu^{178} was modified by the 3,4-epoxybutyl derivative. The active-site residues Glu^{86} and Glu^{177} in *T. reesei* Xyn II are similarly modified, confirming earlier X-ray crystallographic data [Havukainen, Törrönen, Laitinen and Rouvinen (1996) Biochemistry **35**, 9617–9624]. The inability of the ω-epoxyalkyl xylo(oligo)saccharide derivatives to inactivate family-10 enzymes is discussed in terms of different ligand–subsite interactions.

Key words: affinity labelling, enzyme mechanism, glycanases, mass spectrometry, peptide analysis.

INTRODUCTION

Enzymic degradation of the hemicellulolytic part of biomass is a complex process which over the last decade has attracted significant attention due to a number of industrial applications [1]. In most cases, the glycosidase catalytic mechanism involves two essential carboxyl residues: a proton donor and a nucleophile. X-ray analysis (e.g. [2]), irreversible active-site-directed inhibitors (e.g. [3–5]), mutagenesis (e.g. [6,7]), or combinations of these are frequently applied to identify the amino acid residues involved.

The xylanases of glycoside hydrolase families 10 and 11 (EC 3.2.1.8), as classified on the basis of similarity of their amino acid sequences [8–10], can be differentiated further by their catalytic properties [11–14] and structure [2,15,16]. Family-10 enzymes exhibit less strict glycone specificity since cellobiosides, lactosides and D-glucopyranosyl β(1,4)-D-xylopyranosides containing a cleavable aglycone are hydrolysed with considerable turnover numbers [11]. At low substrate concentrations, family-11 enzymes readily show transglycosidation activities [1,13], whereas those from family 10 appear to be strictly solvolytic under these conditions (P. Ntarima, unpublished work); at high substrate concentrations substantial transfer activities have been observed with the xylanase from *Cryptococcus albidus* [17].

The importance of two completely conserved and catalytically important glutamate residues in family-11 glycoside hydrolases [2,18] has been demonstrated previously by site-directed mutagenesis [6,7]. On the basis of the hydrogen-bond network surrounding Glu^{86} in the three-dimensional structure of the xylanase II from *Trichoderma reesei*, it was deduced that this is the nucleophile, Glu^{177} being the acid/base catalyst [19]. Similarly, two conserved glutamate residues are involved in family-10 glycoside hydrolases [20], and a structural study has been published of the Cex xylanase from *Cellulomonas fimi* with the nucleophile catalyst labelled as 2-deoxy-2-fluoro-glycosyl enzyme intermediates [21,22].

Epoxyalkyl glycosides used as affinity-labelling compounds for the relevant glycoside hydrolases are a target for nucleophilic attack [5], yielding a covalent ester bond with a catalytic residue, as shown in Scheme 1. The covalent trapping of three ω-epoxyalkyl D-xylopyranosides into the active site of *T. reesei* Xyn II has been used in a three-dimensional structure determination of these complexes [23]; no detailed kinetic data for these inactivation reactions have been presented.

In the present study, ω-epoxyalkyl glycosides of D-xylopyranose and of xylo-oligosaccharides are shown to only deactivate enzymes from family 11. We report further kinetic analysis of the inactivation, and identification of the modified residues by MS, not only for this enzyme but also for a xylanase from *Thermomyces lanuginosus*, the structure of which has recently been elucidated [24]. The methods of glycanase active-site labelling, peptide digestion and identification of the modified amino acid residues by electrospray ionization MS (ESI-MS) have been described by us previously [25].

Abbreviations used: CNP, 2-chloro-4-nitrophenol; ESI-MS, electrospray ionization MS; DP, degree of polymerization; HPAEC-PAD, high-performance anion-exchange chromatography with pulsed amperometric detection; LC, liquid chromatography.

[1] To whom correspondence should be addressed (e-mail marc.claeyssens@rug.ac.be).

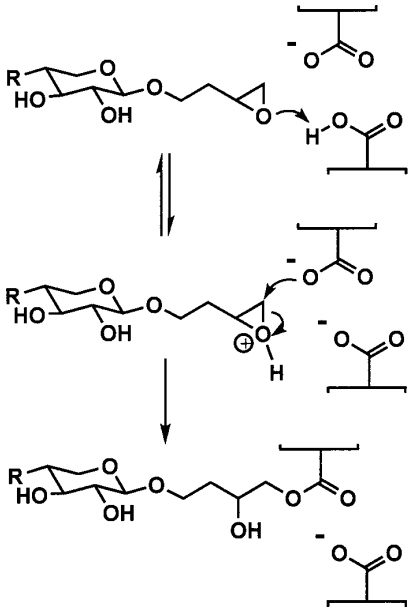

Scheme 1 Mechanism of glycoside hydrolase inhibition by epoxyalkyl glycosides

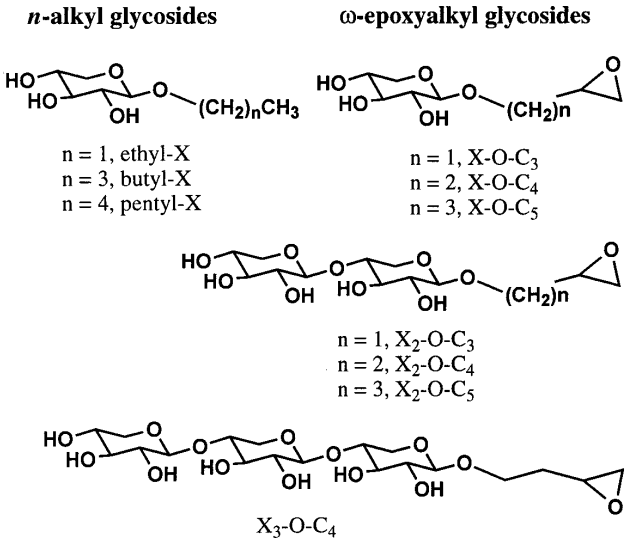

Figure 1 Structures of n-alkyl and derived ω-epoxyalkyl compounds as ligands of xylanases

Ethyl-X, ethyl β-D-xylopyranoside; butyl-X, butyl β-D-xylopyranoside; pentyl-X, pentyl β-D-xylopyranoside; X-O-C_3, 2,3-epoxypropyl β-D-xylopyranoside; X-O-C_4, 3,4-epoxybutyl β-D-xylopyranoside; X-O-C_5, 4,5-epoxypentyl β-D-xylopyranoside; X_2-O-C_3, 2,3-epoxypropyl β-xylobioside; X_2-O-C_4, 3,4-epoxybutyl β-xylobioside; X_2-O-C_5, 4,5-epoxypentyl β-xylobioside; X_3-O-C_4, 3,4-epoxybutyl β-xylotrioside.

EXPERIMENTAL

Substrates, ligands and enzymes

The (*R*,*S*)-ω-epoxyalkyl β-xylo(oligo)saccharides and the n-ethyl, n-butyl and n-pentyl β-D-xylopyranosides used in this study (Figure 1), as well as the chromogenic substrate 2-chloro-4-nitrophenyl β-xylobioside and n-pentyl β-D-galactopyranoside, have been prepared in the laboratory. All monosaccharide derivatives were synthesized as described previously [23,26]. The β-xylo(oligo)saccharide derivatives were synthesized via selective anomeric deprotection of the peracetyl-oligosaccharide [27], coupling with the corresponding γ-alkenol or with 2-chloro-4-nitrophenol (CNP) by the trichloroacetimidate procedure [28], epoxidation of the double bond with *m*-chloroperoxybenzoic acid, and Zemplen acetate deprotection (W. Nerinckx, unpublished work). D-Xylose, xylobiose and xylotriose were commercial (Megazyme, Cork, Ireland) or were isolated from an enzymically prepared oligosaccharide mixture. The *T. lanuginosus* and *Thermoascus aurantiacus* xylanases were purified as described in [1,29]. Xyn II from *T. reesei* was purified by Törrönen et al. [30] and was a gift from Professor J. Rouvinen (Univeristy of Joensuu, Joensuu, Finland). Xyn Z from *Clostridium thermocellum* [31] was donated kindly by Dr P. Béguin (Institut Pasteur, Paris, France).

Inactivation, protection and competitive inhibition experiments

Sets of reaction mixtures containing different concentrations of the epoxides (0–10 mM for monosaccharides, 0–1 mM for oligosaccharides) and a constant concentration of enzyme (0.5 μM) in a total volume of 100 μl were incubated at 25 °C in either 50 mM phosphate buffer at pH 6.4 for *T. lanuginosus* and *C. thermocellum* xylanases, or 50 mM sodium acetate buffer at pH 5.6 for *T. reesei* and *T. aurantiacus* xylanases. At 30 min intervals, 10 μl aliquots taken for activity measurements were added to a solution of 2-chloro-4-nitrophenyl β-xylobioside (200 μl; 500 μM) as substrate, and the product formation (CNP, 405 nm) was followed continuously at 20 °C in a microplate reader (SLT Labinstruments Easy Reader SFplus). The activity of an enzyme blank (without epoxide) was followed in the same way. Apparent inactivation constants were obtained and the relevant association ($1/K_i$) and inactivation (k_i) constants were calculated by conventional analysis of the data [32]. Since the pure diastereoisomers were not available, the stereospecificity of the epoxide inhibitors could not be evaluated.

3,4-Epoxybutyl β-xylotrioside was hydrolysed enzymically and this was monitored by high-performance anion-exchange chromatography with pulsed amperometric detection (HPAEC-PAD; Dionex DX-500 with ED-40 gold electrode detector), injecting 20 μl samples on an anion-exchange column (Carbopac PA-100, 4 mm × 250 mm). A sodium acetate gradient (20–200 mM in 60 mM sodium hydroxide) was applied during 45 min at a flow rate of 1 ml/min. Hydrolysis products were compared with standards (D-xylopyranose, xylobiose and xylotriose) eluted under the same conditions.

Active-site protection experiments were performed with a constant concentration of epoxide inhibitor (1 mM) and enzyme (0.5 μM), and with varying concentrations of the protecting competitive ligand. Activity measurements were performed spectrophotometrically as described above.

Competitive inhibition experiments were performed with varying inhibitor concentration (0–10 mM), two constant substrate concentrations (200 μM and 300 μM; 2-chloro-4-nitrophenyl β-xylobioside with the family-11 enzymes and 2-chloro-4-nitrophenyl β-cellobioside with the family-10 enzymes) and constant enzyme concentration (0.5 μM) in phosphate buffer at pH 6.4. The substrate (200 μl) was added to the enzyme (10 μl) and the liberation of CNP was measured as described above. The results were analysed conventionally [32].

Peptide analysis

Native and inactivated xylanases (45 pmol/μl) were digested overnight with pepsin (enzyme/substrate, 1:20, w/w) in a 50 mM sodium phosphate buffer, pH 2.5, at room temperature. The liquid chromatography (LC)-ESI-MS interface used for analysis and purification of the resulting peptides has been described elsewhere [25]. Separation on a narrow-bore column (2.1 mm × 150 mm) packed with YMC-AQ C_{18} reverse-phase material (5 μm particle size, 120 Å pore size; YMC, Wilmington, NC, U.S.A.) was achieved using 0.05 % (v/v) trifluoroacetic acid containing 5 % acetonitrile (solvent A) and 0.05 % trifluoroacetic acid in 80 % (v/v) acetonitrile (solvent B). A linear gradient of 2–30 % solvent B in 40 min followed by a linear increase to 80 % solvent B in 10 min at a flow rate of 150 μl/min was used, and the freeze-dried peptide samples were analysed by ESI-MS.

MS

Analyses were carried out on a triple quadrupole mass spectrometer (Bio-Q upgraded to the Quattro version, Micromass, Manchester, U.K.) equipped with a pneumatically assisted electrospray source. The instrument was calibrated using the multiple charged ions from an acquisition of bovine trypsinogen at a resolution of which the peak at m/z 1714 was 1 atomic mass unit wide at 50 % above the base line. The proteins were diluted to a final concentration of 5–10 pmol/μl in 50 % acetonitrile containing 0.1 % formic acid, prior to introduction into the source at a flow rate of 5 μl/min. For the nano-electrospray, typically a 1–5 μl sample was sprayed from gold-coated borosilicate glass capillaries (Protana Company, Odense, Denmark). Background-subtracted spectra were processed to convergence using a maximum entropy algorithm (Maxent, part of the Masslynx software from Micromass) and a resolution of 0.5 Da/channel.

Nano-ESI-MS/MS of peptides isolated from preparative LC-ESI-MS analysis of pepsin-digested xylanases was performed by collision-induced dissociation of the singly charged molecular ions using argon and a collision-energy offset of −37 V. Freeze-dried peptides were redissolved in 10 μl of 50 % (v/v) methanol containing 0.05 % formic acid. Approximately 1 μl was loaded into the nanospray capillary. For LC-ESI-MS analysis, the mass spectrometer was scanned from m/z 390 to 1800 in 6 s and the total ion current was recorded. Following acquisition, the base-peak-intensity chromatogram was reconstructed. The resolution was adjusted to resolve the monoisotopic peaks from poly(ethylene glycol) (average mass 2000 Da) to 20 % above the baseline at m/z 1840.

RESULTS AND DISCUSSION

Specificity and kinetics of epoxide-inactivation with family-11 glycoside hydrolases

As an example, the inactivation kinetics of the *T. lanuginosus* xylanase by 3,4-epoxybutyl β-xylobioside are shown in Figure 2. Semi-logarithmic plotting of the residual activity against time is shown in Figure 2(b), giving the values of the apparent rate constants (k_i) for different inhibitor concentrations. For each enzyme and epoxide, the inactivation constants (k_i', K_i) were calculated graphically either by hyperbolic (Figure 2c) or linear (Figure 2d) fitting of the data obtained [32]. The results are summarized in Table 1.

Both the aglycone chain length and the degree of polymerization (DP) of the glycone influence the affinity of the epoxyalkyl derivative. With constant aglycone chain length, the apparent association and inactivation constants increase from D-xylopyranose to xylotriose; these are one order of magnitude higher for the xylobiose and xylotriose derivatives with respect to the results obtained with the monosaccharide derivatives. With the constant DP of the glycone a decrease from propyl to pentyl side chains is observed. In the case of the *T. lanuginosus* xylanase, this holds for all epoxides used, but *T. reesei* Xyn II shows anomalous behaviour with ω-epoxypentyl derivatives: 4,5-epoxypentyl β-xylobioside has a very low affinity, and the inactivation with 4,5-epoxypentyl β-D-xylopyranoside is too slow for adequate measurements. Both family-11 enzymes investigated in this study hydrolyse 3,4-epoxybutyl β-xylotrioside at both glycosidic linkages (see below).

Protection experiments were performed with both enzymes. Varying concentrations of D-xylose, xylobiose (0–10 mM), n-ethyl, n-butyl and n-pentyl β-D-xylopyranoside and n-pentyl β-D-galactopyranoside (0–5 mM) were added to the epoxide-containing mixtures. Xylobiose and the n-alkyl β-D-xylopyranosides did effectively protect, whereas neither D-xylose nor n-pentyl β-D-galactopyranoside did. A representative protection experiment is shown in Figure 3. These protections must be due to a competitive binding at the enzymes' subsites −1 and −2, where the recognition of the glycone moiety (−2) of the epoxide (−1) occurs prior to covalent trapping (subsite labelling according to the −n, +n nomenclature, with −n at the non-reducing end and +n at the reducing end of the oligosaccharide derivative, and cleavage occurring between the −1 and +1 subsites [33]). All above-mentioned ligands are indeed characterized as competitive inhibitors except D-xylose and n-pentyl β-D-galactopyranoside (Table 2). The association constants decrease with increasing n-alkyl chain length, and xylobiose has a low but significant inhibitory power.

Epoxide inactivations are not observed with family-10 glycoside hydrolases

The three-dimensional structure of both β-1,4-glycoside hydrolases from family 10 used in this study (*T. aurantiacus* xylanase and *C. thermocellum* xylanase Z) have been determined [34–36]. The structures of family-10 enzymes are of the $(\alpha/\beta)_8$ TIM-barrel type with the general shape of an elliptical cylinder, showing a deep active-site cleft across the barrel-top along the minor elliptical axis. The polar aromatic residues around the active site are highly conserved, as is a line-up of negative charges within the cleft [34]. In all known family-10 structures [22,34–39], the length of the cleft is about 30 Å, suggesting the presence of 6 (maximum 7) subsites. Subsite-mapping studies have been published for *Pseudomonas fluorescens* subsp. *cellulosa* xylanase A and *C. fimi* Cex [40], and for the *C. albidus* xylanase [41], which show that the subsite-binding energies are highest in subsites −2 and +2, in that order, with a relatively lower (even non-existent with *C. albidus* [41]) contribution from subsite −3. A crystal-structure analysis and subsite mapping of the xylanase from *Penicillium simplicissimum* soaked with xylo-oligosaccharides has been published recently [39]; examination of the three-dimensional data from the complexes reveals that a xylosyl moiety occupying the −3 subsite is substantially exposed to the solvent. The plus subsite region of family-10 enzymes shows considerable variation and might extend to even a +4 subsite in the *P. fluorescens* xylanase [40]. However, a recent competitive assay with xylo-oligosaccharides suggests this enzyme to contain only five major subsites for binding xylan xylosyl units [42].

In striking contrast with the family-11 enzymes, the family-10 glycoside hydrolases from *T. aurantiacus* and *C. thermocellum* were inactivated by none of the epoxyalkyl-derived xylo(oligo)-

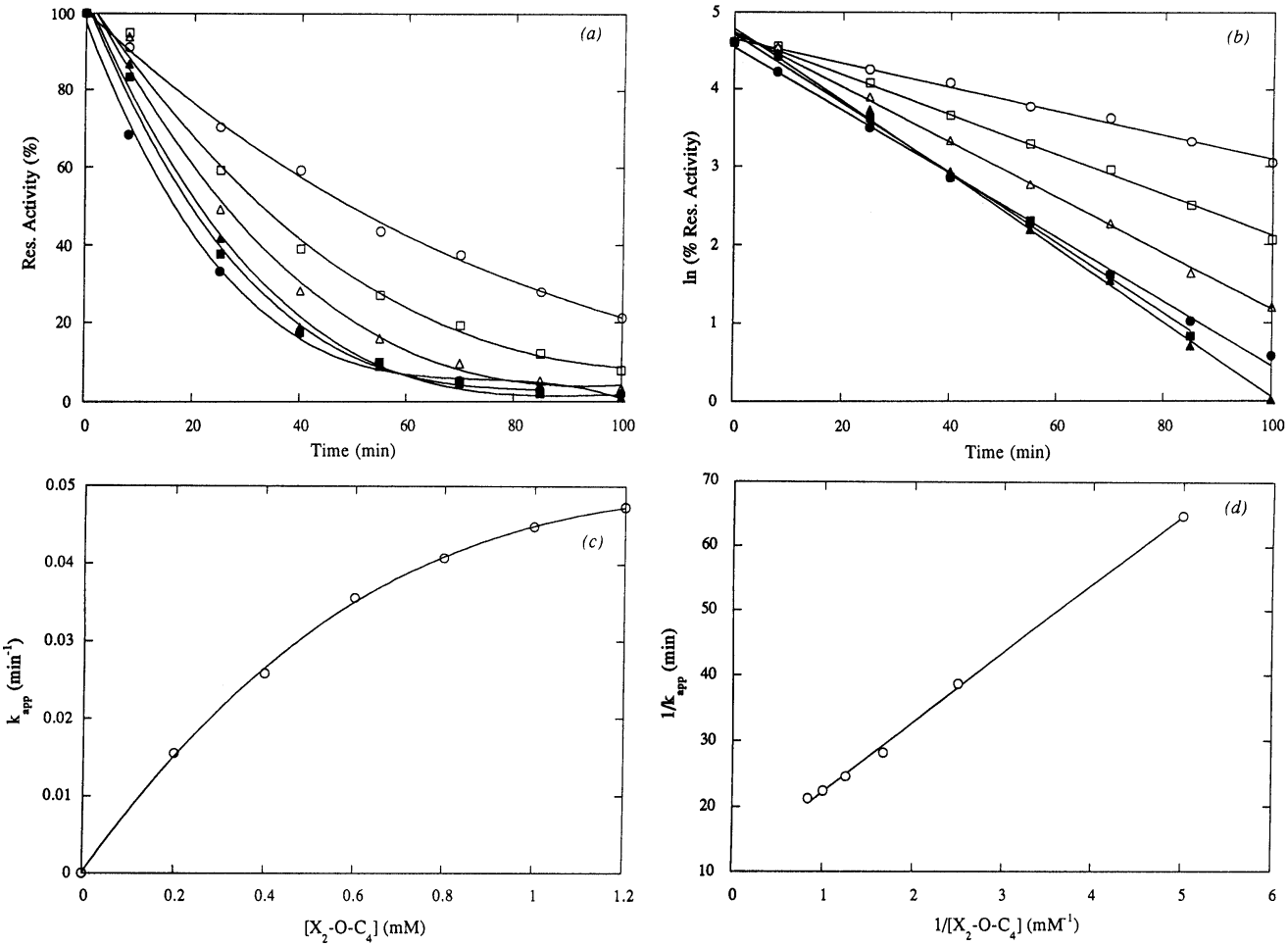

Figure 2 Inactivation kinetics of the *T. lanuginosus* xylanase with 3,4-epoxybutyl β-xylobioside (X_2-O-C_4)

(**a**) Residual activity as a function of time and inhibitor concentration. The enzyme (0.5 μM) was incubated with different concentrations of 3,4-epoxybutyl β-xylobioside [0.2 mM (○), 0.4 mM (□), 0.6 mM (△), 0.8 mM (●), 1.0 mM (■) and 1.2 mM (▲) in 50 mM phosphate buffer, pH 6.4, at 25 °C]. Samples were withdrawn at the indicated time intervals for measurement of residual (Res.) activity. (**b**) Semi-logarithmic plot. (**c**) Hyperbolic plot. (**d**) Linearized plot.

Table 1 Inactivation of the xylanases from *T. lanuginosus* and *T. reesei* (Xyn II)

Association constants ($1/K_i$; M^{-1}) and inactivation rates (k_i; min^{-1}) were determined for the alkyl epoxides derived from D-xylose, xylobiose and xylotriose. X-O-C_3, 2,3-Epoxypropyl β-D-xylopyranoside; X-O-C_4, 3,4-epoxybutyl β-D-xylopyranoside; X-O-C_5, 4,5-epoxypentyl β-D-xylopyranoside; X_2-O-C_3, 2,3-epoxypropyl β-xylobioside; X_2-O-C_4, 3,4-epoxybutyl β-xylobioside; X_2-O-C_5, 4,5-epoxypentyl β-xylobioside; X_3-O-C_4, 3,4-epoxybutyl β-xylotrioside; n.d., not determined.

	X-O-C_3	X-O-C_4	X-O-C_5	X_2-O-C_3	X_2-O-C_4	X_2-O-C_5	X_3-O-C_4
*T. lanuginosus**							
$1/K_i$	140 ± 20	90 ± 50	60 ± 10	1520 ± 200	1090 ± 100	570 ± 90	1280 ± 200
k_i	0.041	0.086	0.0074	0.054	0.086	0.032	0.067
T. reesei†							
$1/K_i$	330 ± 30	290 ± 30	n.d.	4550 ± 400	2630 ± 300	60 ± 20	4170 ± 400
k_i	0.024	0.052	n.d.	0.03	0.043	0.026	0.013

* At pH 6.4 and 25 °C.
† At pH 5.6 and 25 °C.

saccharides, even at high concentration and with prolonged incubation times. Although an epoxide opening by water within the active site is theoretically possible, via protonation of the epoxide functionality by the acid/base catalyst and subsequent nucleophilic attack of a residual water molecule, this is not observed (TLC analysis).

Inhibition experiments showed that the n-alkyl D-xylopyranosides are recognized as competitive ligands (Table 2). In

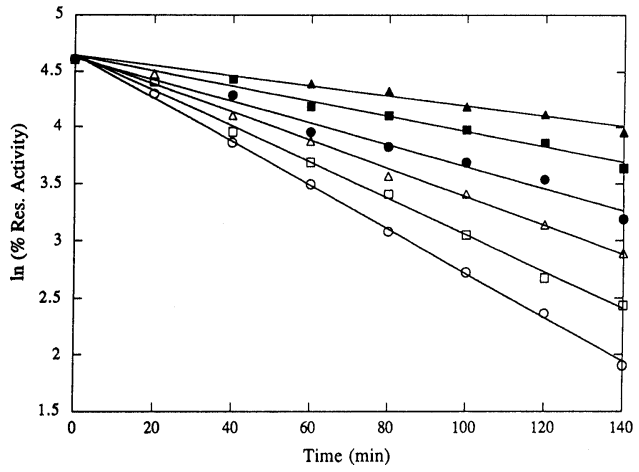

Figure 3 Inactivation of *T. reesei* Xyn II with 2,3-epoxypropyl β-xylobioside in the presence of varying concentrations of n-butyl β-D-xylopyranoside

Semi-logarithmic plot of residual (Res.) activity as a function of time and protector concentration. The enzyme (0.5 μM) was incubated with 2,3-epoxypropyl β-xylobioside (1 mM) and with different concentrations of n-butyl β-D-xylopyranoside [0 mM (○), 1 mM (□), 2 mM (△), 3 mM (●), 4 mM (■), 5 mM (▲) in 50 mM sodium acetate buffer, pH 5.6, at 25 °C]. Samples were withdrawn at the indicated time intervals for measurement of residual activity.

Table 2 Competitive inhibition of family-10 and -11 xylanases

Association constants ($1/K_i$; M^{-1}) were determined for n-alkyl β-D-xylopyranosides and for xylobiose. Ethyl-X, ethyl β-D-xylopyranoside; butyl-X, butyl β-D-xylopyranoside; pentyl-X, pentyl β-D-xylopyranoside.

	Ethyl-X	Butyl-X	Pentyl-X	Xylobiose
Family 11*				
T. lanuginosus Xyn	390 ± 30	190 ± 11	180 ± 17	50 ± 4
T. reesei Xyn II	670 ± 85	440 ± 40	380 ± 30	80 ± 6
Family 10†				
T. aurantiacus Xyn	180 ± 13	500 ± 50	600 ± 72	No inhibition
C. thermocellum Xyn Z	120 ± 7	170 ± 12	260 ± 21	No inhibition

* With 2-chloro-4-nitrophenyl β-xylobioside as substrate.
† With 2-chloro-4-nitrophenyl β-cellobioside as substrate.

contrast with the family-11 enzymes, the association constants increase with increasing chain length. Surprisingly, in our study xylobiose is completely ineffective as inhibitor with both family-10 enzymes, although a weak competitive inhibition ($K_{i(app)}$ 105 mM) was observed recently with the *P. fluorescens* xylanase A [42]. In our case, the observed inhibitions of the n-alkyl D-xylopyranosides can be envisaged as arising from binding at the plus subsites. Indeed, a recognition at the −1 (alkyl) and −2 (xylose) subsites is unlikely, because in that case the analogous ω-epoxyalkyl derivatives, when binding at the −1 (epoxide) and −2 (xylose) subsites, should be effective inactivators. Instead, the D-xylose unit of n-alkyl D-xylopyranosides presumably interacts with the +2 subsite, being the second in order of binding-energy contribution (see the published subsite-affinity studies of this family [39,41]). The very weak affinity of xylobiose is then explained by a repulsive interaction of a xylose moiety for the enzymes' +1 subsite, and a possible interaction of xylobiose with the product subsites +2 and +3 is then too low for observation by inhibition experiments. This could indicate a built-in mechanism for product removal, a property that is also suggested in the recent structural study describing the subsite mapping of the *P. simplicissimum* xylanase [39], where, in addition, the soaking experiment with only xylobiose showed exclusive occupation of the −1 and −2 subsites, suggesting that xylobiose in the *P. fluorescens* xylanase A is also recognized at the minus, not the plus, subsites. Also, the fact that transglycosidation activity with family-10 enzymes is only observed at high substrate concentrations ([17], and P. Ntarima, unpublished work) can be explained by poor ligand recognition at the plus subsites. Inverting this rationale, one can expect substantial product inhibition at the plus subsites with those enzymes that are known to have good glycosyl-transferring properties.

Since ω-epoxyalkyl xylo(oligo)saccharide inactivations, which must occur via prior recognition of the carbohydrate moiety by the minus subsites, could not be observed with family-10 enzymes (in contrast with those of family 11), these enzymes apparently also have a relatively poor ligand-recognition capability at the minus subsites (in comparison with those of family 11); that is, for short xylo-oligosaccharides in all-chair conformations. Still, family-10 enzymes show Michaelis–Menten parameter values of the usual magnitude for xylo-oligosaccharides of DP 4 or higher [39,41,43]. For productive substrate recognition of a long xylo-oligosaccharide, concomitant binding with the plus and minus subsites must then be necessary, including strong compensating interactions at the enzyme–substrate complex which have yet to be observed in structural studies. In this respect, it is noteworthy to point to a conserved tryptophan residue [34,38,44] situated above the −1 subsite (e.g. Trp^{281} in the Cex xylanase from *C. fimi* [21]), which shows some degree of flexibility as compared with the overall rigidity of the cleft-like active site of family-10 enzymes [21,34,36–38,44–46]. As a unique feature of these enzymes, this residue is found on the lower tip of a thumb-like extended loop often containing a small α-helix portion, residing above the $(\alpha/\beta)_8$ barrel and pointing inwards to the active site. It can be envisaged that this tryptophan adopts a specific substrate-enclosing position at the stage of the critical enzyme–substrate complex, thereby improving the enzyme's fit with a distorted substrate [22,47,48] on its route along the reaction coordinate. Such interaction would be less prominent with (alkyl derivatives of) mono- and disaccharides presented to the active site. The function of Trp^{276} as a 'lid' has also been discerned in the above-reported *P. simplicissimum* xylanase subsite-mapping study [39]. Unfortunately, no complexes with an intact glycosidic bond between subsites −1 and +1 could be obtained, and the authors found no apparent evidence of this Trp^{276} influencing the position of the catalytic residues. Nevertheless, its role in substrate recognition must be pivotal. Indeed, a site-directed mutagenesis study of xylanase A from *S. lividans* [44] showed that replacement of the equivalent Trp^{274} substantially decreases k_{cat} for hydrolysis of birchwood xylan, suggesting that this residue plays a key role in stabilization of the catalytic intermediate.

MS analysis of labelling specificity of family-11 glycoside hydrolases

ESI-MS analyses of the two family-11 glycoside hydrolases, either intact or modified with the three ω-epoxyalkyl derivatives of D-xylopyranose, gave evidence for single conjugate species formation. In Figure 4 are shown the ESI-MS spectra of the *T. lanuginosus* xylanase before (Figure 4, top panel) and after

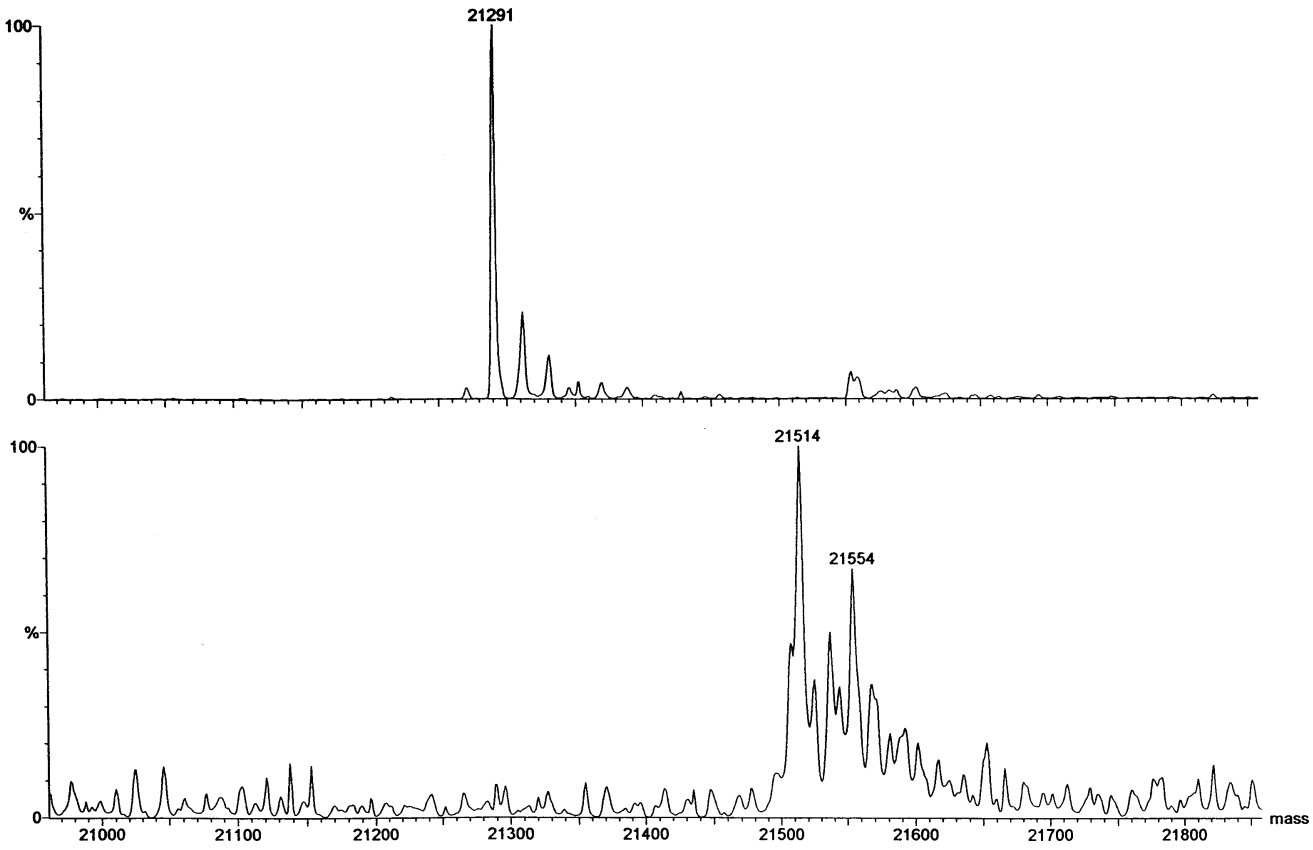

Figure 4 Deconvoluted mass spectra of the *T. lanuginosus* xylanase

(Top panel) Before derivatization with 3,4-epoxybutyl β-D-xylopyranoside; (bottom panel) after derivatization.

Table 3 Summarized results from ESI-MS analysis of *T. reesei* Xyn II and *T. lanuginosus* Xyn before and after modification with ω-epoxyalkyl derivatives

X-O-C_3, 2,3-epoxypropyl β-D-xylopyranoside; X-O-C_4, 3,4-epoxybutyl β-D-xylopyranoside; X-O-C_5, 4,5-epoxypentyl β-D-xylopyranoside; X_2-O-C_3, 2,3-epoxypropyl β-xylobioside; X_2-O-C_4, 3,4-epoxybutyl β-xylobioside; X_3-O-C_4, 3,4-epoxybutyl β-xylotrioside.

	M_r					
	Before	Calculated	Inhibitor (M_r)	Observed M_r after activation	ΔM_r	Conjugate found
T. reesei Xyn II	20822.8	20825	X-O-C_3 (206.2)	21026.8 ± 6.81	204.0	X-O-C_3
			X-O-C_4 (220.2)	21041.4 ± 2.54	218.6	X-O-C_4
			X_2-O-C_3 (338.3)	21163.8 ± 5.79	341.0	X_2-O-C_3
			X_2-O-C_4 (352.3)	21172.9 ± 1.27	350.1	X_2-O-C_4
			X_3-O-C_4 (484.4)	21043.1 ± 1.86	220.3	X-O-C_4
			X_3-O-C_4 (484.4)	21175.4 ± 1.16	352.6	X_2-O-C_4
			X_3-O-C_4 (484.4)	21391.9 ± 1.71	569.1	X-O-C_4 + X_2-O-C_4
			X-O-C_5 (234.2)	21063.4 ± 1.10	240.5	X-O-C_5
T. lanuginosus Xyn	21292.9	21290	X-O-C_3 (206.2)	21498.5 ± 5.37	205.6	X-O-C_3
			X-O-C_4 (220.2)	21514.1 ± 2.10	221.2	X-O-C_4
			X_2-O-C_3 (338.3)	21496.2 ± 6.27	303.3	X-O-C_3
			X_2-O-C_3 (338.3)	21630.3 ± 4.10	337.4	X_2-O-C_3
			X_2-O-C_4 (352.3)	21642.8 ± 1.11	349.9	X_2-O-C_4
			X_3-O-C_4 (484.4)	21775.6 ± 6.07	482.7	X_3-O-C_4
			X_3-O-C_4 (484.4)	21510.4 ± 6.84	217.5	X-O-C_4
			X_3-O-C_4 (484.4)	21646.3 ± 4.34	353.4	X_2-O-C_4
			X_3-O-C_4 (484.4)	21863.3 ± 5.93	570.4	X-O-C_4 + X_2-O-C_4

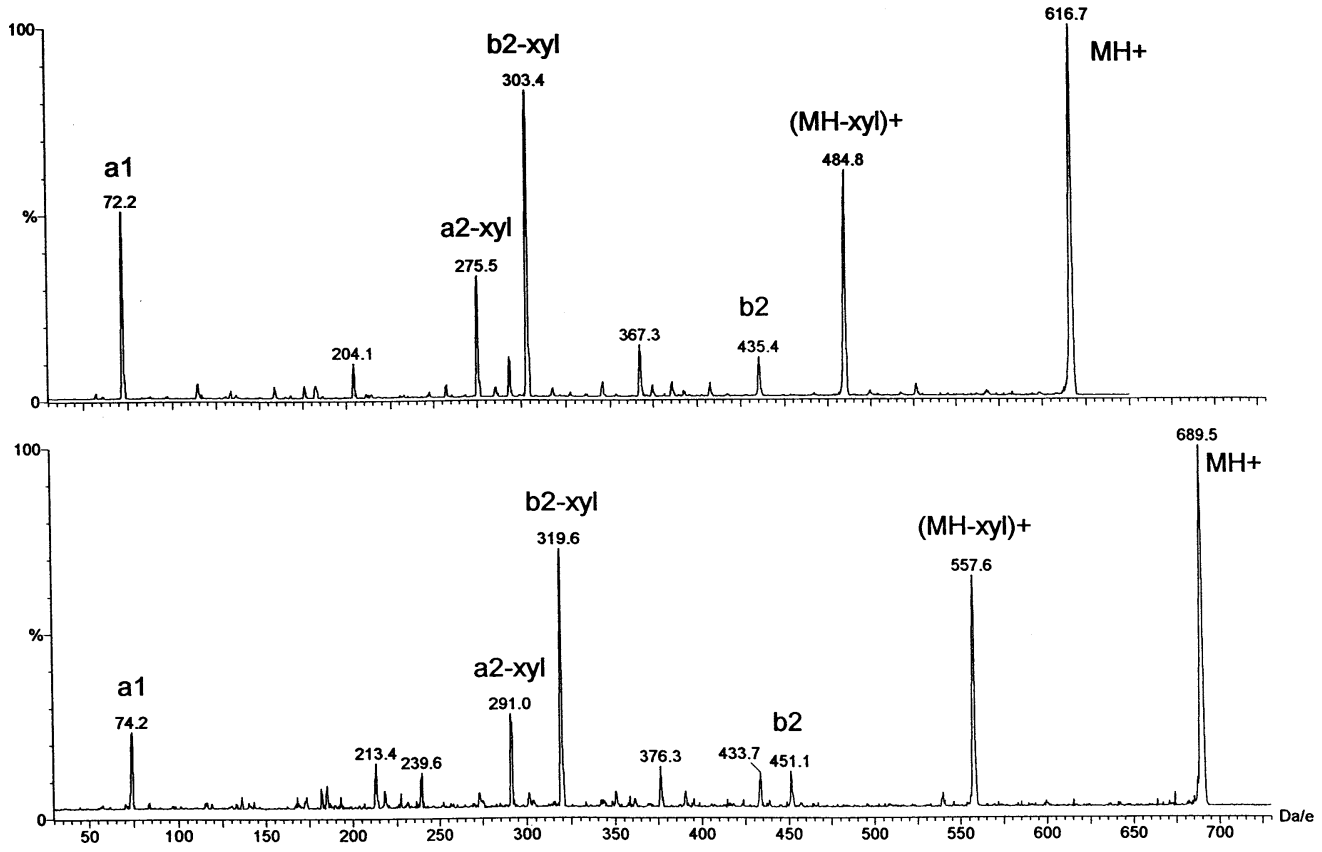

Figure 5 Nano-ESI-MS/MS spectra of the isolated peptides from the *T. lanuginosus* xylanase

Peptide was labelled with (top panel) 2,3-epoxypropyl β-D-xylopyranoside or (bottom panel) 3,4-epoxybutyl β-D-xylopyranoside. The peak labels refer to fragment ions as shown in Table 4 and Figure 6. Da/e, dalton/electronic charge; xyl, xylose.

(Figure 4, bottom panel) modification with epoxybutyl β-D-xylopyranoside; the apparent mass shift of 223 Da corresponds well to the theoretical addition of 220 Da expected for covalent attachment of a single 3,4-dihydroxybutyl xylopyranoside molecule. The observed lower-intensity peaks probably correspond to potassium adducts.

Samples treated with the xylobioside derivatives also show single conjugate species, except in the case of the *T. lanuginosus* xylanase where the propyl derivative apparently can be hydrolysed and two species with the corresponding mass for the monoside and bioside conjugates were found.

The enzyme samples inactivated with 3,4-epoxybutyl β-D-xylotrioside contained several species showing single (mono-, di- or trisaccharide) or double (mono- and disaccharide) labelling. These must have resulted from hydrolysis at both glycosidic linkages of the trisaccharide before labelling of an active-site residue, leading to a mixture of epoxybutyl mono-, di- and trisaccharides. Double labelling then presumably occurred both at the active site and unspecifically at some other carboxylate residue. The hydrolysis of 3,4-epoxybutyl β-D-xylotrioside was confirmed by HPAEC-PAD analysis of the reaction mixture after 1 h: two new eluates corresponding to xylose and xylobiose clearly emerged (results not shown).

The results of the ESI mass analyses of *T. reesei* Xyn II and *T. lanuginosus* Xyn before and after modification with different epoxyalkyl derivatives are summarized in Table 3.

MS analysis of modified peptide digests of family-11 glycoside hydrolases

The peptides derived from pepsin digestion of *T. reesei* Xyn II and *T. lanuginosus* xylanase, which were inactivated with epoxypropyl and 3,4-epoxybutyl β-D-xylopyranoside, were isolated by preparative LC-ESI-MS. The amino acid residues modified by the affinity label were identified unambiguously using nano-ESI-MS/MS. The detailed results with the epoxypropyl- and epoxybutyl β-D-xylopyranoside-inactivated *T. lanuginosus* enzyme are presented in Figures 5 and 6 and in Table 4.

A mixture of the 2,3-epoxypropyl and the 3,4-epoxybutyl β-D-xylopyranoside-derivatized *T. lanuginosus* xylanase was digested overnight with pepsin. As compared with the capillary LC-MS chromatogram of the pepsin digest of intact enzyme, the one obtained from the labelled peptide mixture revealed two new main eluting compounds. These peptides were isolated and subsequently analysed by nano-ESI MS/MS. Figure 5 shows the spectra of the 2,3-epoxypropyl and 3,4-epoxybutyl β-D-xylopyranoside modified peptides from the *T. lanuginosus* xylanase, corresponding to ^{85}VEY^{87} (MH^+ 616.7) and ^{177}TEGY^{180} (MH^+ 689.5) respectively. Next to the protonated molecular ion MH^+, both peptides also show the ion resulting from the loss of the xylopyranoside moiety ($MH^+ -$ xylose: 484.6 and 556.5 respectively). Of the calculated expected N-terminal fragment ions (Table 4), in both peptides a non-labelled a1 fragment is observed

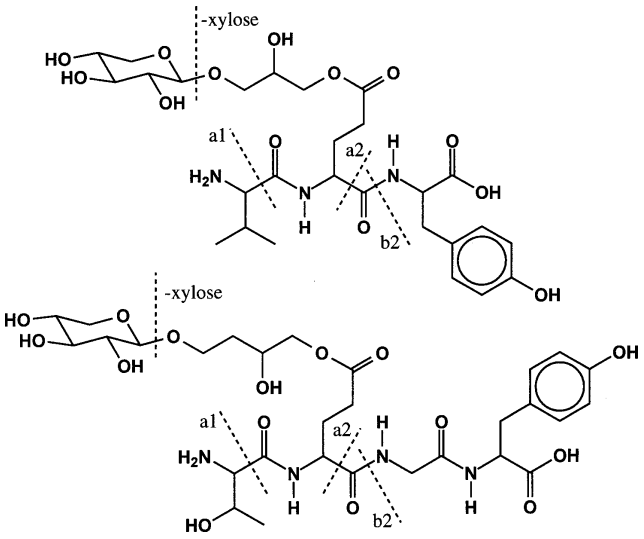

Figure 6 Modified peptide structures from the *T. lanuginosus* xylanase

Top: Val-Glu-Tyr (VEY) modified by 2,3-epoxypropyl β-D-xylopyranoside (M_r 616.7). Bottom: Thr-Glu-Gly-Tyr (TEGY) modified by 3,4-epoxybutyl β-D-xylopyranoside (M_r 689.5) as revealed by ESI-MS/MS. Fragmentation sites are indicated.

Table 4 Calculated N-terminal side-chain fragment ions of the Val-Glu-Tyr (VEY)-epoxypropyl and Thr-Glu-Gly-Tyr (TEGY)-epoxybutyl β-D-xylopyranoside-derivatized peptides from *T. lanuginosus* xylanase

For side-chain fragment ion nomenclature see [49,50]. Values in bold indicate observed ions.

	Modified VEY-peptide				Modified TEGY-peptide			
	Val^{85}	Glu^{86}	Tyr^{87}		Thr^{177}	Glu^{178}	Gly^{179}	Tyr^{180}
Fragment	1	2	3	Fragment	1	2	3	4
a	**72.1**	201.2	364.4	a	**74.1**	203.2	260.3	423.5
+74.1	145.2	**274.3**	437.5	+88.1	165.2	**291.3**	348.4	511.6
+206.2	278.3	407.4	570.6	+220.3	294.4	423.5	480.6	643.8
b	100.1	229.2	392.7	b	102.1	321.2	288.3	451.5
+74.1	174.2	**303.3**	466.8	+88.1	190.2	**319.3**	376.4	539.6
+206.2	306.3	**435.4**	598.9	+220.3	322.4	**451.5**	508.6	671.8
MH^+ − xylose: **484.6**; MH^+: **616.7**				MH^+ − xylose: **556.5**; MH^+: **689.8**				

plus the tell-tale a2 and b2 fragments containing respectively the epoxypropyl and butyl moieties (+74.1 and +88.1), and especially the b2 fragments, each containing an intact affinity label (+206.2 and +220.3). This fragmentation pattern unequivocally proves the specific epoxypropyl-Glu^{86} versus epoxybutyl-Glu^{178} labelling (Figure 6).

The ESI-MS/MS ion fragment analysis for the labelled *T. reesei* digests indicated ^{85}IEY^{87} (MH^+ 630.7) and ^{176}VEGY^{179} (MH^+ 687.9) as the respective 2,3-epoxypropyl and 3,4-epoxybutyl β-D-xylopyranoside-modified peptides, and shows the analogous a1 and modified b2 fragment ions as above.

Our results confirm a previous X-ray diffraction study with ω-epoxyalkyl β-D-xylopyranosides in which the nucleophile Glu^{86} and the acid/base catalyst Glu^{177} were also seen as the modified residues; the former with 2,3-epoxypropyl and 4,5-epoxypentyl β-D-xylopyranoside, the latter with 3,4-epoxybutyl β-D-xylopyranoside [23]. This study also revealed an anti-Markovnikov epoxide opening in all cases, i.e. the nucleophilic attack of the acid/base catalyst has occurred on the primary carbon of the epoxide functionality, and not on the secondary carbon, although this pathway would have yielded the more stable secondary carbonium-ion intermediate. Epoxide trapping at the primary carbon probably occurred for steric reasons, an important observation that was not noticed by the authors. The differential specificity of proton donor versus nucleophile of the enzymes towards alkyl epoxides of different chain lengths is not unsurprising in view of the mechanism, since, upon protonation of the epoxide by the proton donor, nucleophilic attack may occur by the enzyme's original nucleophile or by the now deprotonated acid/base catalyst (Scheme 1). A protonated epoxide functionality within the active site may have a lifetime long enough to allow for reorientation of the flexible alkyl chain, and is eventually trapped by the best-positioned glutamate residue.

Conclusion

Inactivations with ω-epoxyalkyl derivatives of D-xylose, xylobiose and xylotriose point to specific interactions of these ligands at the minus subsites with concomitant modification of either the general acid/base catalyst (in the case of the epoxybutyl derivative) or the nucleophile (in the case of the epoxypropyl derivative) in the active sites of glycoside hydrolases from family 11.

For the family-10 enzymes these inhibitors are inefficient. An alternative binding, presumably at the plus subsites, is corroborated by inhibition studies with either xylobiose or n-alkyl D-xylosides. The pivotal role in substrate recognition of a conserved tryptophan residue situated above the −1 subsite is suggested.

We are indebted to Dr Pierre Béguin (Institut Pasteur, Paris, France) and Professor J. Rouvinen (University of Joensuu, Joensuu, Finland) for generous gifts of enzymes. M.C. and M.K.B. are indebted to the European Union for Copernicus (CIPA-CT94 0232) and Inco-Copernicus (IC-CT96-1000) grants.

REFERENCES

1 Bennet, N. A., Ryan, J., Biely, P., Vršanská, M., Kremnicky, L., Macris, B. J., Kekos, D., Christakopoulos, P., Claeyssens, M., Nerinckx, W. et al. (1998) Carbohydr. Res. **306**, 445–455
2 Davies, G. and Henrissat, B. (1995) Structure **3**, 853–859
3 Nitta, Y., Isoda, Y., Toda, H. and Sakiyama, F. (1989) J. Biochem. (Tokyo) **105**, 573–576
4 Macarron, R., Van Beeumen, J., Henrissat, B., de la Mata, I. and Claeyssens, M. (1993) FEBS Lett. **316**, 137–140
5 Withers, S. G. and Aebersold, R. (1995) Protein Sci. **4**, 361–372
6 Svensson, B. and Søgaard, M. (1993) J. Biotechnol. **29**, 1–37
7 Wakarchuk, W. W., Campbell, R. L., Sung, W. L., Davoodi, J. and Yaguchi, M. (1994) Protein Sci. **3**, 467–475
8 Henrissat, B. (1991) Biochemistry **280**, 309–316
9 Henrissat, B. and Bairoch, A. (1993) Biochem. J. **239**, 781–788
10 Henrissat, B. and Bairoch, A. (1996) Biochem. J. **316**, 695–696
11 Claeyssens, M. and Henrissat, B. (1992) Protein Sci. **1**, 1293–1297
12 Biely, P., Kluepfer, D., Morosoli, R. and Shareck, F. (1993) Biochim. Biophys. Acta **1162**, 246–254
13 Törrönen, A. and Rouvinen, J. (1997) J. Biotechnol. **57**, 137–149
14 Biely, P., Vršanská, M., Tenkanen, M. and Kluepfel, D. (1997) J. Biotechnol. **57**, 151–166
15 Coutinho, P. M. and Henrissat, B. (1999) in Recent Advances in Carbohydrate Bioengineering (Gilbert, H. J., Davies, G., Henrissat, B. and Svensson, B., eds.), pp. 3–12, The Royal Society of Chemistry, Cambridge
16 Coutinho, P. M. and Henrissat, B. (1999) in Genetics, Biochemistry and Ecology of Cellulose Degradation (Ohmya, K., Hayashi, K., Sakka, K., Kobayashi, Y., Karita, S. and Kimura, T., eds.), pp. 15–23, Uni Publishers Co., Tokyo
17 Biely, P., Vršanská, M. and Krátký, Z. (1981) Eur. J. Biochem. **119**, 565–571
18 Törrönen, A., Kubicek, C. P. and Henrissat, B. (1993) FEBS Lett. **321**, 135–139
19 Törrönen, A., Harkki, A. and Rouvinen, J. (1994) EMBO J. **13**, 2493–2501

20 Gebler, J. C., Gilkes, N. R., Claeyssens, M., Wilson, D. B., Béguin, P., Wakarchuk, W. W., Kilburn, D. G., Miller, R. C., Warren, R. A. J. and Withers, S. G. (1992) J. Biol. Chem. **267**, 12559–12561
21 White, A., Tull, D., Johns, K., Withers, S. G. and Rose, R. R. (1996) Nat. Struct. Biol. **3**, 149–154
22 Notenboom, V., Birsan, C., Rose, D. R., Warren, R. A. J. and Withers, S. G. (1998) Nat. Struct. Biol. **5**, 812–818
23 Havukainen, R., Törrönen, A., Laitinen, T. and Rouvinen, J. (1996) Biochemistry **35**, 9617–9624
24 Gruber, K., Klintschar, G., Hayn, M., Schlacher, A., Steiner, W. and Kratky, C. (1998) Biochemistry **37**, 13475–13485
25 Klarskov, K., Piens, K., Stahlberg, J., Hoj, P. B., Van Beeumen, J. and Claeyssens, M. (1997) Carbohydr. Res. **304**, 143–154
26 De Bruyne, C. K. and Loontiens, F. G. (1966) Nature (London) **209**, 396–397
27 Ferrer Sabat, C., Exero Agnesti, P. and Bemporad Caniato, M. (1976) Spanish Patent 430 636, Laboratories Ferrer S. L
28 Schmidt, R. R. and Jung, K.-H. (1997) in Preparative Carbohydrate Chemistry (Hanessian, S., ed.), pp. 283–308, Marcel Dekker, New York
29 Bhat, M. K., Parry, N. J., Kalogiannis, S., Beever, D. E., Owen, E., Nerinckx, W. and Claeyssens, M. (1998) in Carbohydrases from *Trichoderma reesei* and Other Organisms; Proceedings of the Tricel '97 meeting held in Ghent, Belgium, 28–31 August 1997 (Claeyssens, M., Nerinckx, W. and Piens, K., eds.), pp. 102–112, The Royal Society of Chemistry, Cambridge
30 Törrönen, A., Harkki, A. and Kubicek, C. P. (1992) Bio/Technology **10**, 1461–1465
31 Grépinet, O., Chebrou, M.-C. and Béguin, P. (1988) J. Bacteriol. **170**, 4576–4581
32 Segel, I. H. (1975) Biochemical Calculations, pp. 208–323, Wiley & Sons, Chichester
33 Davies, G. J., Wilson, K. S. and Henrissat, B. (1997) Biochem. J. **321**, 557–559
34 Natesh, R., Bhanumoorthy, P., Vithayathil, P. J., Sekar, K., Ramakumar, S. and Viswamitra, M. A. (1999) J. Mol. Biol. **288**, 999–1012
35 Lo Leggio, L., Kalogiannis, S., Bhat, M. K. and Pickersgill, R. W. (1999) Proteins Struct. Funct. **36**, 295–306
36 Dominguez, R., Souchon, H., Spinelli, S., Dauter, Z., Wilson, K. S., Chauvaux, S., Beguin, P. and Alzari, P. M. (1994) Nat. Struct. Biol. **2**, 569–576
37 Derewenda, U., Swenson, L., Green, R., Wei, Y., Morsoli, R., Shareck, F., Kleupfel, D. and Derewenda, Z. S. (1994) J. Biol. Chem. **269**, 20811–20814
38 Harris, G. W., Jenkins, J. A., Connerton, I., Cummings, N., Lo Leggio, L., Scott, M., Hazlewood, G. P., Laurie, J. I., Gilbert, H. J. and Pickersgill, R. W. (1994) Structure **2**, 1107–1116
39 Schmidt, A., Gübitz, G. M. and Kratky, C. (1999) Biochemistry **38**, 2403–2412
40 Charnock, S. J., Spurway, T. D., Xie, H., Beylot, M.-H., Virden, R., Warren, R. A. J., Hazlewood, G. P. and Gilbert, H. J. (1998) J. Biol. Chem. **273**, 32187–32199
41 Biely, P., Krátký, Z. and Vršanská, M.(1981) Eur. J. Biochem. **119**, 559–564
42 Lo Leggio, L. and Pickersgill, R. W. (1999) Enzyme Microb. Technol. **25**, 701–709
43 Bray, M. R. and Clarke, A. J. (1992) Eur. J. Biochem. **204**, 191–196
44 Roberge, M., Shareck, F., Morosoli, R., Kluepfel, D. and Dupont, C. (1999) Protein Eng. **12**, 251–257
45 White, A., Withers, S. G., Gilkes, N. R. and Rose, D. R. (1994) Biochemistry **33**, 12546–12552
46 Schmidt, A., Schlacher, A., Steiner, W., Schwab, H. and Kratky, C. (1998) Protein Sci. **7**, 2081–2088
47 Sinnott, M. L. (1990) Chem. Rev. **90**, 1171–1202
48 Withers, S. G. (1999) Can. J. Chem. **77**, 1–11
49 Roepstorff, P. and Fohlman, J. (1984) Biomed. Mass Spectrom. **11**, 601–616
50 Biemann, K. (1989) in Protein Sequencing: a Practical Approach (Findlay, J. B. C. and Geisow, M. J., eds.), pp. 99–118, IRL Press, Oxford

Received 7 October 1999/26 January 2000; accepted 23 February 2000